

INVERSION OF ULTRASONIC ATTENUATION FOR TEXTURAL INFORMATION OF POLYCRYSTALS

S. Ahmed and Tom Taylor

Pacific Northwest National Laboratory, Richland, WA, USA

Abstract: The mechanical properties of polycrystalline materials depend on the individual physical properties of the constituent grains. When grains are randomly oriented with respect to a fixed coordinate system, the average elastic properties are isotropic. A polycrystalline aggregate possesses macroscopic texture, and thus exhibit anisotropic elastic properties, when the grains are preferentially oriented. Accurate knowledge of texture is important for a number of engineering applications. For example, it plays an important role in determining their subsequent formability into finished parts of complex shape by deep drawing. Textural information can also be exploited to assess plastic damage in a component due to fatigue or external impact. Current ultrasonic methods are based on the relationship between ultrasonic phase velocities and only the low-order orientation distribution coefficients (ODCs, a set of orthonormal basis functions to express crystallographic orientation of a grain), a consequence of the application of Voigt averaging method to infer aggregate elastic properties. Thus, such techniques provide only a partial description of texture. It is well-known from the scattering theories that while phase velocity of acoustic waves is controlled primarily by averages of single grain elastic constant fluctuations, attenuation due to scattering of such waves at the grain boundaries are controlled by two-point averages of these fluctuations. Since these two-point averages depend on higher order ODCs, inversion of measured attenuation is expected to yield a more complete and accurate description of texture. In this paper, we will present computed frequency and direction dependent attenuation coefficient of ultrasonic waves in orthotropic polycrystals with equiaxed cubic grains and mathematically investigate the inversion of computed attenuation coefficient to obtain higher order ODCs. We will also compute pole figures and compare them with those obtained by current ultrasonic methods.

Introduction: A polycrystalline material is composed of numerous discrete grains, each having a regular, crystalline atomic structure. The elastic properties of the grains are anisotropic and their crystallographic axes are oriented differently. When an acoustic wave propagates through such a polycrystalline aggregate, it is attenuated by scattering at the grain boundaries, with the value of this attenuation and the related shift in the propagation velocity depending on the size, shape, orientation distributions, and crystalline anisotropy of the grains. If the grains are equiaxed and randomly oriented, these propagation properties are independent of direction, but such is not the case when the grains are elongated and/or have preferred crystallographic orientation. Therefore, reliable ultrasonic testing of engineering alloy components require the knowledge of the anisotropies in the attenuation and velocities of ultrasonic waves due to preferred grain orientations and elongated shapes.

The propagation of elastic waves in randomly oriented, equiaxed polycrystals has received considerable attention, with most recent contributions for the cubic materials being made by Hirsekorn [1,2] Stanke and Kino [3,4], Beltzer and Brauner [5], and Turner [6]. Stanke and Kino present their “unified theory” based on the second order Keller approximation [7] and the use of a geometric autocorrelation function to describe the grain size distribution. Stanke and Kino argue that their approach is to be preferred because i) the unified theory more fully treats multiple scattering, ii) the unified theory avoids the high frequency oscillations which are coherent artifacts of the single-sized, spherical grains assumed by Hirsekorn, and iii) the unified theory correctly captures the high frequency “geometric regime” in which the Born approximation breaks down. The theoretical treatment of ultrasonic wave propagation in preferentially

oriented grains is more limited. Hirsekorn has extended her theory to the case of preferred crystallographic orientation while retaining the assumption of spherical grain shape [8], and has performed numerical calculations for the case of stainless steel with fully aligned [001] axes [9]. Turner, on the other hand, derives the Dyson equation using anisotropic Green's functions to predict the mean ultrasonic field in macroscopically anisotropic medium [6]. He then proceeds to obtain the solution of the Dyson equation for the case of equiaxed grains with aligned [001] axes.

Previously Ahmed and Thompson [10, 11] have employed the formalism of Stanke and Kino [3, 4] in [001] aligned stainless steel polycrystal to compute the mean attenuation and phase velocity of plane ultrasonic waves. The effects of grain scattering on mean/expected acoustic waves are controlled by the so-called one- and two-point averages which depend on the orientation distribution of the individual grains. It is customary to represent these orientations by the ODCs [12]. In this paper we first compute the expected wave vector in a macroscopically orthotropic polycrystalline material with cubic grains. Next, we proceed to show how one can proceed to invert the attenuation data for twelve ODCs by using the computed attenuation. We choose polycrystalline iron for our calculations with orthotropic symmetry. Table 1 shows the single crystal physical properties. The twelve ODCs employed in our calculations are listed in Table 2.

Table 1. Material properties

Material	$c_{11} (N/m^2)$	$c_{12} (N/m^2)$	$c_{44} (N/m^2)$	$\rho (kg/m^3)$
Iron	21.6×10^{10}	14.5×10^{10}	12.9×10^{10}	7.86×10^3

Table 2. Orientation distribution coefficients

	l = 4	l = 6	l = 8
W_{l00}	-6.702024×10^{-3}	4.7245817×10^{-3}	-2.183566×10^{-4}
W_{l20}	$-1.4832119 \times 10^{-3}$	$-1.4903041 \times 10^{-3}$	6.3966168×10^{-4}
W_{l40}	1.6121439×10^{-3}	5.7128322×10^{-4}	$-1.4337244 \times 10^{-3}$
W_{l60}		1.738688×10^{-4}	$-1.0366931 \times 10^{-3}$
W_{l80}			$-4.8526059 \times 10^{-4}$

Theory: The displacement field due to an ultrasonic wave propagating in a polycrystalline material can be described by the stochastic wave equation

$$[C_{ijkl}^{\xi}(\mathcal{P})u_{kl}^{\xi}(\mathcal{P})]_{,j} + \rho^{\xi}(\mathcal{P})\omega^2 u_i^{\xi}(\mathcal{P}) = 0, \quad (1)$$

where $C_{ijkl}^{\xi}(\mathcal{P})$ is the actual local elastic tensor, $\rho^{\xi}(\mathcal{P})$ is the actual local density, and $u_i^{\xi}(\mathcal{P})$ is the actual displacement field in the medium ξ . The set of elastic tensors and the probability density function $p(\xi)$, which is the probability of choosing any particular medium, form a stochastic process. In a medium with no density variation, the application of the unified theory of Stanke and Kino [3] to the

wave equation yields the generalized following Christoffel's equation for the expected propagation constant k .

$$[\Gamma_{ik} - \rho\omega^2 / k^2 \delta_{ik}] = \mathfrak{D} \quad (2a)$$

where

$$\Gamma_{ik} = \hat{k}_j \hat{k}_l \{ C_{ijkl}^o + \varepsilon \langle \Delta_{ijkl} \rangle + \varepsilon^2 [\langle \Delta_{ij\alpha\beta} \Delta_{\gamma\delta kl} \rangle - \langle \Delta_{ij\alpha\beta} \rangle \langle \Delta_{\gamma\delta kl} \rangle] \int G_{\alpha\gamma}(\mathfrak{P}) [W(\mathfrak{P}) e^{i\mathfrak{k}\mathfrak{P}\cdot\hat{k}}]_{,\beta\delta} d^3\mathfrak{P} \}, \quad (2b)$$

$\varepsilon \Delta_{ijkl} = C_{ijkl}(\mathfrak{P}) - C_{ijkl}^o$, $G_{\alpha\gamma}(\mathfrak{P})$ is a Green's function taken from the work of Lifshits and Parkhamovski [13], C_{ijkl}^o are the unweighted Voigt [14] averaged elastic constants, and $W(\mathfrak{P})$ represents the geometric autocorrelation function (the probability that two points, placed randomly in the material and separated by a displacement \mathfrak{P} , fall in the same crystallite). Equation (2) describes the expected propagation constant k of plane waves of the form $\langle u_i \rangle = \hat{a} \hat{u} e^{-i\mathfrak{k}\mathfrak{P}\cdot\hat{k} - i\omega t}$, where ω is the angular frequency and $\hat{k} = k\hat{k}$ is the propagation vector in the direction of propagation \hat{k} . k is related to phase velocity v and attenuation coefficient α through the relationship $k = \omega / v - i\alpha$.

Equation (2) admits solutions for \hat{u} only if the determinant of the matrix in brackets on the left-hand side vanishes. In the absence of scattering, these occur for three distinct real values of ω^2 / k^2 ; one for each of the two quasi-shear waves and one for the quasi-longitudinal wave. In the presence of scattering, requiring the determinant to vanish defines a transcendental equation which may support many roots. The correct root was selected by seeking the real part of the root closest to the root in the absence of scattering and requiring that the imaginary part $\alpha \geq 0$. The wave polarizations are given by the corresponding eigenvectors.

In this paper, we only consider polycrystals with equiaxed grains and use the following geometric autocorrelation function $W(\mathfrak{P})$ proposed by Stanke and Kino [3].

$$W(\mathfrak{P}) = e^{-2s/d} \quad (3)$$

where d is the mean grain diameter. Following the general procedure to obtain the complex propagations constants and polarizations as described before, we were able to develop an integral equation for the expected propagation constant for elastic waves propagating along the rolling, the transverse, and the normal directions. As elastic waves along these directions are purely longitudinal or shear, we only need, for example in the case of propagation in the 3-direction, the averages $\varepsilon \langle \Delta_{3333} \rangle$ and

$\varepsilon^2 [\langle \Delta_{33kl} \Delta_{mn33} \rangle - \langle \Delta_{33kl} \rangle \langle \Delta_{mn33} \rangle]$ in our calculations. The averages are calculated in the following manner [12].

If f is a function of the orientation of a crystallite whose Euler angles are (θ, ψ, ϕ) , then

$$\langle f \rangle = \int_0^{2\pi} \int_{-1}^1 \int_0^{2\pi} f(\xi, \psi, \phi) w(\xi, \psi, \phi) d\psi d\xi d\phi, \quad \xi = \cos \theta, \quad w(\xi, \psi, \phi) = \sum_{l=0}^{\infty} \sum_{m=-l}^l \sum_{n=-l}^l W_{lmn} Z_{lmn}(\xi) \quad (4)$$

In these expressions, W_{lmn} are the ODCs and Z_{lmn} are the Legendre polynomials. For equiaxed grains, integration required in equation (2) were performed analytically, thus resulting in a highly nonlinear algebraic equation for the expected propagation constant k .

Results and Discussions: To obtain the attenuation per wavelength α / k_o and the normalized shift in phase velocity $(v - v_o) / v_o$ for plane waves in the considered textured medium, the equation for the expected propagation constants, algebraic equation resulting from Equation (2) after carrying out the integration, was solved numerically. Here and in what follows, v_o and k_o refer to phase velocity and wave number, respectively, based on unweighted Voigt averaged elastic constants. The subscripts 'l' and 's' associated with the Voigt averaged quantity refer to L- and S-waves, respectively. The single crystal elastic constants used for the polycrystalline iron are listed in Table 1. The twelve ODCs required in the evaluation of the averages $\varepsilon < \Delta_{ijkl} >$ and $\varepsilon^2 [< \Delta_{ijkl} \Delta_{mnpq} > - < \Delta_{ijkl} > < \Delta_{mnpq} >]$ are shown in Table 2.

Normalized frequency ($k_o d$) dependence of the normalized attenuation coefficients and phase velocities of L-waves for propagation in the rolling, transverse, and normal directions are shown in figures 1 and 2. The shape of these curves characterizing different frequency regimes (Rayleigh, stochastic, and geometric) are similar to those corresponding to untextured polycrystals [1][2][3]. It is interesting to note that the ripples observed in Hirsekorn's calculations [8] in the transition between the Rayleigh and the stochastic regions are absent in the present calculations. This is to be expected since different grain sizes and shapes are taken into account in the unified theory of Stanke and Kino.

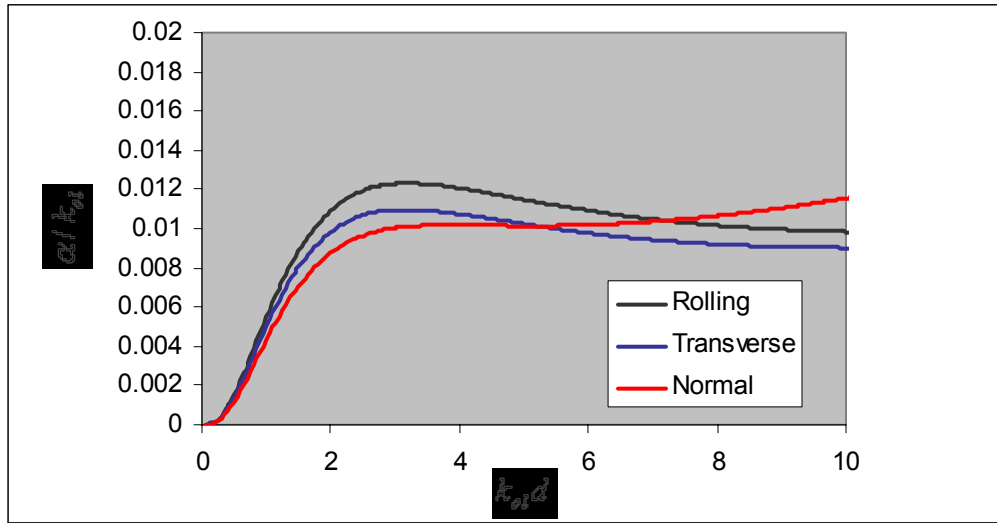


Figure 1. Frequency dependence of normalized attenuation coefficients for L-waves.

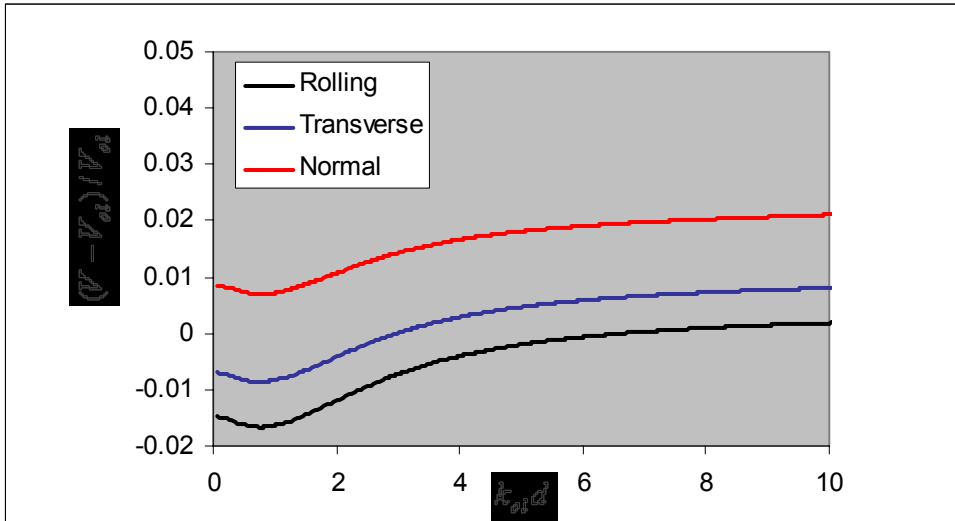


Figure 2. Frequency dependence of normalized phase velocities for L -waves.

Figures 3 and 4 show the variation of attenuation coefficients and normalized phase velocities with normalized frequency ($k_{os} d$) of shear waves propagating in the rolling direction with polarizations in the transverse and normal directions.

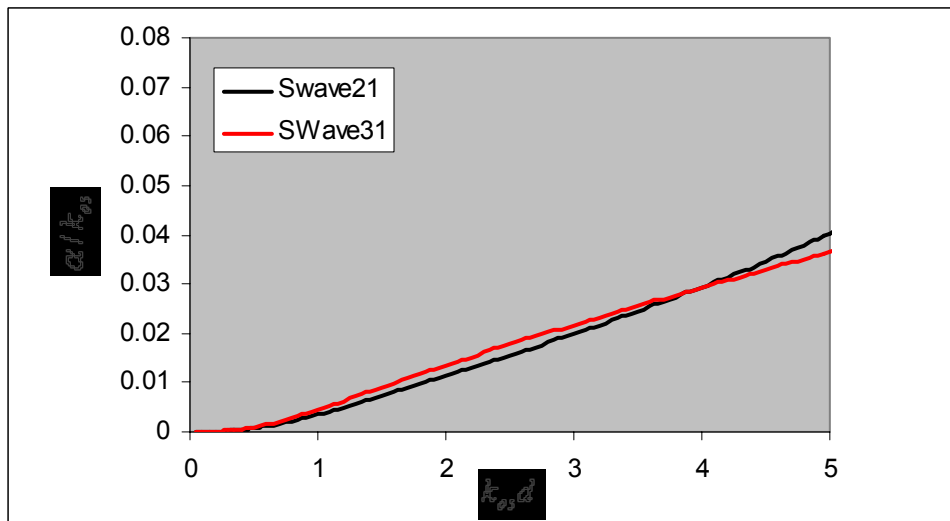


Figure 3. Frequency dependence of normalized attenuation coefficients for S -waves propagating in the rolling direction.

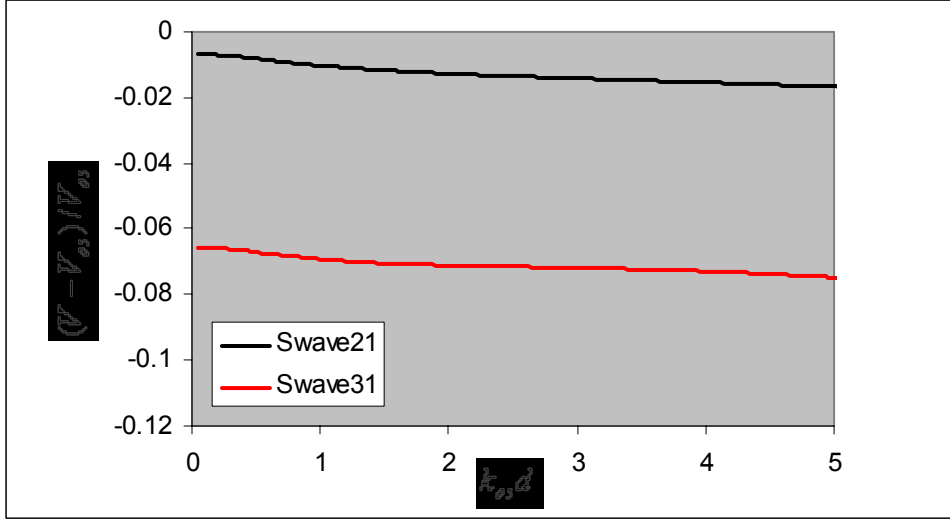


Figure 4. Frequency dependence of normalized phase velocities for S -waves propagating in the rolling direction.

As a first step towards inverting the attenuation data for ODCs, we are in the process of performing a numerical experimentation where we assume the mean grain size and compute the expected complex wave number k for L - and S -waves in different directions, using the data listed in tables 1 and 2. This inversion process is not yet complete but a very simple procedure has shown us the feasibility of such inversions. For example, when we consider L -wave propagation in the normal direction, it is noted that the ODCs that appear in equation 2 through the one- and two-point averages are W_{400} , W_{420} , W_{440} , W_{600} , W_{620} , W_{640} , W_{800} , W_{820} , and W_{840} . Inversion of the predicted attenuation assuming W_{400} to be the only nonzero ODC yields the value -6.936×10^{-3} for W_{400} which compares well with the actual value of -6.702024×10^{-3} . Use of this value for W_{400} in inverting attenuation data for shear wave propagating in the normal direction with polarization in the rolling direction under the assumption that the only other nonzero ODC is W_{420} yields the value -1.64×10^{-3} for W_{420} which also compares well with the actual value of $-1.4832119 \times 10^{-3}$. Similar simple inversion algorithm when applied to shear wave propagating in the normal direction with polarization in the transverse direction gives $W_{440} = 1.5813 \times 10^{-3}$ as opposed to the actual value of 1.6121439×10^{-3} . Continuing in this fashion, we compute other ODCs that appear in the expression for attenuation for L -waves propagating in the normal direction. Finally, we minimize the difference in simulated inverted ODCs and the input ODCs for a given propagation direction. For example, if we chose the normal direction to be the propagation direction for L -waves, we obtain the following for the ODCs. It is to be noted that the ODCs W_{660} , W_{860} , and W_{880} do not appear in the expression for attenuation of L -waves propagating in the normal direction.

	Input	Computed
W_{400}	-6.702024×10^{-3}	-6.71845×10^{-3}
W_{420}	$-1.4832119 \times 10^{-3}$	-1.48793×10^{-3}
W_{440}	1.6121439×10^{-3}	1.55645×10^{-3}
W_{600}	4.7245817×10^{-3}	5.21197×10^{-5}
W_{620}	$-1.4903041 \times 10^{-3}$	1.27340×10^{-4}
W_{640}	5.7128322×10^{-4}	-3.44665×10^{-5}
W_{800}	-2.183566×10^{-4}	1.19537×10^{-4}
W_{820}	6.3966168×10^{-4}	1.20958×10^{-4}
W_{840}	$-1.4337244 \times 10^{-3}$	1.42733×10^{-4}

The computed values of other ODCs have considerable errors and hence are not included in this paper.

Conclusions: We have applied the unified theory of Stanke and Kino [3] to determine the propagation constants in a textured polycrystalline material and used it to explore the feasibility of inverting measured attenuation for ODCs. Our initial inversion shows that the lower order ODCs can be quite accurately predicted from attenuation measurements. It is hoped that the use of a more robust inversion algorithm will reduce the errors in computing the higher order ODCs from attenuation data. Currently, we are developing an inversion algorithm based on genetic algorithm and the results will be published elsewhere at a later time.

Acknowledgement: This work was supported by Department of Energy under Contract DE-AC 06-76RLO 1830.

References:

1. S. Hirsekorn, "The scattering of ultrasonic waves by polycrystals," J. Acoust. Soc. Am., 72, 1021-1031 (1982).
2. S. Hirsekorn, "The scattering of ultrasonic waves by polycrystals. II shear waves," J. Acoust. Soc. Am., 73, 1160-1163 (1983).
3. F. E. Stanke and G. S. Kino, "A unified theory for elastic wave propagation in polycrystalline materials," J. Acoust. Soc. Am., 75, 665-681 (1984).
4. F. E. Stanke, "Unified theory and measurements of elastic waves in polycrystalline materials," Ph. D. thesis, Stanford University, Stanford, CA (1983).
5. I. Beltzer and N. Brauner, "Shear waves in polycrystalline media and modifications of the Keller approximation," Intl. J. Solids Structures, 23, Vol. 1, 201-209 (1987).
6. J. T. Turner, "Elastic wave propagation and scattering in heterogeneous, anisotropic media: Textured polycrystalline materials," J. Acoust. Soc. Am., 106, 541-552 (1999).

7. J. B. Keller, "Stochastic equations and wave propagation in random media," in Proceedings of the 16th Symposium on Applied Mathematics (American Mathematical Society, New York, NY, 1964), pp. 145-179.
8. S. Hirsekorn, "The scattering of ultrasonic waves in polycrystalline materials with texture," J. Acoust. Soc. Am., 77, 832-843 (1985).
9. S. Hirsekorn, "Directional dependence of ultrasonic propagation in textured polycrystals," J. Acoust. Soc. Am., 79, 1269-1279 (1986).
10. S. Ahmed and R. B. Thompson, "Propagation of elastic waves in equiaxed stainless steel polycrystals with aligned [001] axes," J. Acoust. Soc. Am., 99, 2086-2096 (1996).
11. S. Ahmed and R. B. Thompson, "Effect of preferred grain orientation and grain elongation on ultrasonic wave propagation in stainless steel," Review of Progress in Quantitative Nondestructive Evaluation, 11B, pp.1999-2006, Plenum (1992).
12. R. Roe, "Description of Crystallite Orientation in Polycrystalline Materials. III. General Solution to Pole Figure Inversion", J. Appl. Phys. 36, 2024-2031 (1965).
13. E. M. Lifshits and G. D. Parkhamovski, *Zh. Eksperin. Theoret.* 20, 175-182 (1980).
14. W. Voigt, *Lehrbuch der Kristallphysik*, Tauber, Leipzig, 1928, p. 962.